Learning General Features From Images and Audio With Stacked Denoising
Autoencoders.

by

Nathan H. Nifong

A thesis submitted in partial fulfillment of the
requirements for the degree of

Master of Science
in
Systems Science

Thesis Committee:
Wayne Wakeland,
Marty Zwick,
Melanie Mitchell.

Portland State University
2013

Contents

Abstract

One of the most impressive qualities of the brain is its neuro-plasticity. The neocortex has roughly the same structure throughout its whole surface, yet it is involved in a variety of different tasks from vision to motor control, and regions which once performed one task can learn to perform another [15]. Machine learning algorithms which aim to be plausible models of the neocortex should also display this plasticity. One such candidate is the stacked denoising autoencoder (SDA). SDA's have shown promising results in the field of machine perception where they have been used to learn abstract features from unlabeled data. [25, 26, 35] In this thesis I develop a flexible distributed implementation of an SDA and train it on images and audio spectrograms to experimentally determine properties comparable to neuro-plasticity, Specifically, I compare the visual-auditory generalization between a multi-level denoising autoencoder trained with greedy, layer-wise pre-training (GLWPT), to one trained without. I test a hypothesis that networks pre-trained on one sensory modality will perform better on the other modality than randomly initialized networks trained for an equal total number of epochs. Furthermore, I also test the hypothesis that the magnitude of improvement gained from this pre-training is greater when GLWPT is applied than when it is not.

1 Introduction and Background

1.1 Introduction

It is an ongoing effort in machine learning to match the powerful learning capacity of the human brain. Deep belief networks are a recently successful neurally inspired class of machine learning algorithms. In this thesis I set out to investigate the plasticity, or adaptability, of stacked denoising autoencoders, a type of deep belief network. See section 2.6 and figure 3 for an explanation of SDA's. Plasticity gives us an idea of how brain-like the SDA algorithm is. If we seek to make brain-like learning algorithms, using the "intelligence" of those algorithms as a measure of success is both too vague, and too distant to be useful. If we instead look for esoteric behaviors and qualities that we know to be brain-like, such as plasticity, it reveals more readily applicable clues about where to invest our efforts in further research[19]. Following from this motive I measure the plasticity of SDA's by switching models between data from two different sensory modalities, images and audio, and observing the effect on reconstruction accuracy. I test two distinct hypotheses:

1. SDA models trained on one sensory modality and then switched to a second sensory modality half-way through training will have a higher reconstruction accuracy on test data from the second sensory modality than randomly initialized networks trained for an equal total number of epochs on the second sensory modality exclusively.

2. When hypothesis 1 is tested using SDA's trained with greedy layer-wise pre-training vs. SDA's without, the magnitude of the difference in reconstruction accuracy described in hypothesis 1 will be greater for SDA's trained with greedy layer-wise pre-training.

The hypotheses are tested by training stacked denoising autoencoders on an image dataset and an audio dataset with identical dimensionalities. Three variables are manipulated: single or multi-modal training data, layer-wise or interleaved layer training order, and audio or images as the test data. There are 8 experiments in total, each one run with 20 different random seeds. The results indicate that both hypotheses are confirmed with a p-value of ? for hypothesis 1 and a p-value of ? for hypothesis 2. In conclusion I postulate that the GLWPT training helped the SDAs learn abstract features, and this in turn improved its generalizability between different sensory modalities. I address the unexpected small magnitude of differences between reconstruction error between the experimental and control models, and discuss potential causes and fixes. I include visualizations of the features learned and graphs of the reconstruction error over time for each layer in several pairs of models. These figures illustrate interesting unexpected observations about the training process which could be the focus of future work.

1.2   Neural Plausibility of Machine Learning Algorithms

The latest strides in the field of machine learning are coming from deep networks [1, 14, 17, 27, 24, 34]. This class of learning algorithm is inspired by the structure of the mammalian neocortex, specifically the visual areas in the occipital lobe which have been studied more extensively than any other part. This is in contrast to non-neurally inspired algorithms such as support vector machines (SVM) that are more widely used and were notably better at classification than neural networks[3, 8, 29, ?]. Now that we are seeing biologically inspired algorithms leading the way, biological plausibility becomes a useful heuristic for the further development of algorithms with higher performance measures, and discoveries about the emergent properties of these algorithms may feed back into neuroscience to inform further study of the brain. One

metric which defines the brain and differentiates it from other intelligent systems is its plasticity. Areas which once specialized in a certain function can change and learn a new function if for some reason they cannot continue with their first function or if the second function is just much more demanding of computational resources. [33]

1.3   Hierarchical representation in the brain

Deep networks are like the neocortex in many ways, but the most important of them is the hierarchical structure from which they get their name. In the visual cortex, neuroscientists have found using single-neuron recording that there are cells which respond most strongly to specific visual stimuli. The nature of the stimuli which excite the neurons changes changes along many dimensions throughout the visual cortex. One of the more salient dimensions of variation is that of *abstraction*[18]. The organization of the visual cortex is illustrated in figure 1. The cells in V1 are the first cells in the cortex to receive signals from the retina via the lateral genticulate nucleus, a part of the thalamus. Cells here respond most actively to a particular edge at a particular angle within a small area of vision called their receptive field. As one moves up V2, V3, V4, and V5 the cells respond to more and more abstract visual stimuli until one sees cells that do things like activating whenever a dog is in the visual field, when objects appear to be moving in a specific way, and even abstract visual conditions such as "currently looking at object in hand" regardless of what or where it is. While it is possible that each of those abstract stimuli has a large set of neurons dedicated to recognizing it out of a "raw" sensory stream, it's far more plausible that they recognize it out of a small, and information-rich stream of intermediate representations. This leads to the idea that a hierarchical structure is crucial to the functionality of the neocortex.

1.4 The reusability of hierarchical representations.

A hierarchical, or tree-like, structure of knowledge representation allows one to construct compact representations of a massive and complex distribution of stimuli. First one learns that the data can be represented in a slightly more compact way as a finite collection of simple patterns corresponding to local, high-frequency (short-term), salient features in sensory signals. A similar process is applied to the first-level features to construct another set of more abstract features, which can represent the data even more compactly. Thus, one re-uses representations rather than learning a whole new set for each abstract feature. In the case of vision, the levels of a hierarchy of representation might be as follows. Images can all be represented as pixel arrays, And pixel arrays can be represented more compactly as a collection of overlapping gradients, edges, and spots chosen from a finite set, and colored with a small finite set of colors. (This is the principle behind JPEG compression and appears to be the principal organization of the visual striate cortex.[5]) These patches are commonly compared to Gabor filters, depicted in figure 2[6, 23], and are the most commonly learned set of features in machine vision. As one moves up the chain of abstraction in vision, nearly all combinations of edges and spots seen in natural images can be represented even more compactly as a hierarchy of things, stuck to the surfaces of bigger things in roughly specified locations, illuminated from a given angle [12]. Assuming you have a library of hundreds of thousands of things, and the texture of spots, edges, and colors that typically make up their surface, and the ability to calculate shadows, one can decode, or render, this representation into the one below it.

The tricky part of course is learning the vocabularies of symbols that make up each layer and the weights on the connections that allow you to translate between them. Traditional multi-layer neural networks assume pre-set finite number of layers and nodes at each layer, and then attempt to learn the feed-forward weights which connect

layers all at once using back-propagation and Stochastic Gradient Descent (SGD). There are no weights which operate on the information feeding backwards except in some recurrent neural networks. For the most part, pure SGD doesn't work very well. On large networks (hundreds of nodes at each layers and more than 3 layers) the search will get stuck in effective local minima[10, 20].

1.5   Deep networks

Deep networks can have the same structure as traditional neural networks (set number of layers, set number of nodes at each layer, full feed-forward connections, and sigmoid activation function) but they are trained one layer at a time in order to initialize the optimization procedure for higher layers in a good basin of attraction, and they usually employ some kind of dropout in order to enforce sparse hierarchical representations[21, 24]. Dropout is a technique of adding noise to data to promote generalizability over accuracy in lower layers. Classical multilayer neural networks must search the entire weight space with no bias or heuristic. For large enough weight spaces, or noisy enough data, Even the best optimization procedure will become trapped in a local minima. Greedy layer-wise pre-training and dropout both help to provide some structure and bias to the search process to reduce the dimensionality of the space, smooth out it's features and discover better minima. Deep networks have been shown to be able to learn the abstract feature sets that traditional multi-layer neural networks were originally expected to be able to learn[17]. Classical networks can theoretically learn any function, but in practice, they can only learn smooth functions well in a reasonable amount of time.

There are several types of deep belief networks, but they share the property of having layers stackable interfaces. They consist of a number of modules, which can be increased in depth indefinitely. Denoising autoencoders and Boltzmann machines are

commonly used modules[32]. The module serves the purpose of performing gener-
alization, and optionally compression. Each module will re-code it's input to a new
representation, and this representation serves as the input for the next layer. For each
type of module, there are many variants that differ in the method used to learn the
parameters, such as marginalized autoencoders, which are optimized for speed [4]. In
order to use a module within a deep network, the module must meet certain criteria.
It must perform some limited form of generalization, and must operate on the same
format of data it produces, such that it can be stacked recursively. To date, most
modules are feed forward only, but several very interesting generative deep recurrent
neural networks have also been studied[13].

1.6   Stacked denoising autoencoders

The aim of the autoencoder is to learn the code $\mathbf{y}$, a distributed representation that
captures the coordinates along the main factors of variation in the data, $\mathbf{x}$ (similar
to how principal component analysis (PCA) captures the main factors of variation
in the data). An autoencoder takes an input $\mathbf{x} \in [0, 1]^d$ and first maps it (with an
encoder) to a hidden representation $\mathbf{y} \in [0, 1]^{d'}$ through a deterministic mapping with
weights $\mathbf{W}$, e.g.:

$$\mathbf{y} = s(\mathbf{W}\mathbf{x} + \mathbf{b})$$

Where s is a non-linearity such as the sigmoid. The latent representation $\mathbf{y}$, or code
is then mapped back (with a decoder) into a reconstruction $\mathbf{z}$ of same shape as $\mathbf{x}$
through a similar transformation, e.g.:

$$\mathbf{z} = s(\mathbf{W}'\mathbf{y} + \mathbf{b}')$$

9

where ′ does not indicate transpose, and $\mathbf{z}$ should be seen as a prediction of $\mathbf{x}$, given the code $\mathbf{y}$. The parameters of this model (namely $\mathbf{W}$, $\mathbf{b}$, $\mathbf{b}'$ and $\mathbf{W}'$) are optimized such that the average reconstruction error is minimized. When using the traditional squared error measurement, the reconstruction error is defined as :

$$L(\mathbf{x}, \mathbf{z}) = ||\mathbf{x} - \mathbf{z}||^2$$

Because $\mathbf{y}$ is viewed as a lossy compression of $\mathbf{x}$, it cannot be a good compression (with small loss) for all $\mathbf{x}$, so learning drives it to be one that is a good compression in particular for training examples, and hopefully for others as well, but not for arbitrary inputs. That is the sense in which an autoencoder generalizes: it gives low reconstruction error to test examples from the same distribution as the training examples, but generally high reconstruction error to uniformly chosen configurations of the input vector. An auto-encoder is identical to a classical three-layer neural network, with the primary difference being that it attempts to learn the identity function. The vector presented on the input is the same same vector expected on the output. Since the number of nodes in the hidden layer is typically less than that of the input, the network's weights are prevented from simply converging on identity matrices. Essentially, the information storage capacity of the hidden layers is less than that of the input, therefore some compression must occur. There are other, more effective ways of enforcing this compression, but the simplest way is to use fewer hidden nodes than input nodes.

The normal training procedure for an autoencoder is to use stochastic gradient decent (SGD) to minimize the mean squared error in the reconstruction by searching the space of weights on the encoder and decoder's connections. Sometimes the weights are said to be shared, which means the encoder and decoder use the same weights. The purpose of this is to reduce the size of the search space by $1/2$ without having a

severe impact on performance. In the case of shared weights, It is reasonable to say there is not an encoder and a decoder, but simply a nonlinear transformation which is optimized to work well in both directions.

Under some conditions, an autoencoder is isomorphic to PCA. If the activation function is linear (as opposed to sigmoid or tanh) and the mean squared reconstruction error is value minimized, then the network learns to project the input in the span of the first $\mathbf{n}$ principal components of the data, where $\mathbf{n}$ is the width of the hidden code $\mathbf{y}$. If the activation function is non-linear, the autoencoder behaves differently from PCA, with the ability to capture multi-modal aspects of the input distribution. The departure from PCA becomes even more important when we consider stacking multiple encoders (and their corresponding decoders) when building a deep belief network [20]. The autoencoder alone is not sufficient to be the basis of a deep architecture because it has a tendency towards over-fitting, so initial experimentation with deep networks used restricted Boltzmann machines as a basic module instead[32].

The denoising autoencoder (dA) is an extension of a classical autoencoder introduced specifically as a building block for deep networks[35]. It attempts to reconstruct a corrupted version of the input, but the reconstruction, $\mathbf{z}$ is still compared against the uncorrupted input, $\mathbf{x}$. This is known as dropout because random components of the input vector are "dropped". The stochastic corruption process consists in randomly setting some of the numbers in the input vector (as many as half of them) to zero. Hence the denoising autoencoder is trying to predict the corrupted values from the uncorrupted values, for randomly selected subsets of the full input vector. This modification allows the dA to generalize well and produces compounding benefits when the dA's are stacked into a deep network[20]. Geoffrey Hinton suggests that the stochastic timing of the action potentials observed in biological neurons is a similar feature evolved to moderate the potential for over-fitting, and allows neurons or neuron groups to generalize well over the range of activation patterns of their

receptive fields[16].

I have introduced the autoencoder, and the denoising autoencoder. Next I'll explain the stacked de-noising autoencoder and it's benefits over a single denoising autoencoder. A stacked denoising autoencoder is composed of multiple denoising autoencoders where each DA takes the hidden code from the layer below. See figure 3 for a diagram of and SDA. When a new layers is added only after the current highest layer has converged, the network is said to be trained with *greedy layer-wise pre-training* or GLWPT. When all the layers are present from the start, the training is referred to as interleaved. First, a single denoising autoencoder is trained on the data in the usual way by optimizing the weights to minimize the reconstruction error. Its hidden layer converges on a sparse distributed representation of the training set. This essentially replaces the step where a researcher would have to design a collection of good features. Then, a second denoising autoencoder is trained to reconstruct corrupted versions of the activation of the hidden layer of the first dA for the collection of training examples. (the first level does not learn during this time). In an unsupervised learning task where the features, or hidden code of each layer are the desired product, the process is stopped at this point. If the network is to be used for classification or some other supervised learning task, the network is said to be pre-trained at this point and a final step is performed called fine-tuning. During fine-tuning the encoders from the lowest to highest layer are ordered into a network, and an addition new set of weights is created to map the highest level hidden code to an output vector often representing class labels from a supervised training dataset. This whole stack of layers is treated like a classical multi-layer neural network and trained using back-propagation and SGD. The experiments in this thesis do not call for fine-tuning because no labeled data is used.

1.7 Greedy layer-wise pre-training

Why does greedy layer-wise pre-training help deep networks find good solutions? Dumitru Erhan at al. found that greedy layer-wise pre-training acts like a regularizer. [2]

1.8 Relevant work

Brandon Rohrer at Sandia National Laboratories developed a model which learned abstract features from images and audio known as BECCA [31]. It is inspired by the properties of the visual cortex, and attempts to re-create the visual cortex's generality and flexibility. Rohrer postulates that abstract feature discovery may be responsible for the generality and flexibility of the neocortex, but that we don't yet know for certain.

> *Re-routing sensory inputs to a new cortical location results in similar feature creation phenomena, hinting that the cortex may be performing a similar function throughout its extent. If that is the case, the function it performs may be nothing more than feature creation. However, there is still far too little data available to certify or disprove such a statement.*

Honglak Lee et al. applied convolutional deep belief networks to audio classification with notable success [28]. They extracted features from spectrograms of short audio snippets of speech from the TIMIT phoneme dataset, and from music [11]. They were able to perform classification of the artist and the genre of songs, as well as classify phonemes from speech snippets, using the same set of learned features.

Undoubtedly, the most successful applications of deep networks are in the field of machine vision. One example that stands out is the classification of objects from the enormous ImageNet dataset using convolutional deep belief nets by Alex Krizhevsky,

Ilya Sutskever, and Geoffrey E. Hinton[24, 7]. Although they did not perform any unsupervised pre-training, they achieved record breaking classification performance. They also describe the challenges posed by distributing their computation across multiple GPUs.

Dumitru Erhan et al. have investigated why unsupervised pre-training helps stacked denoising autoencoders, and have found that unsupervised pre-training initializes a deep architecture in a basin of attraction of gradient descent corresponding to better generalization performance [9]. They hypothesize that due to the non-convexity of the training criterion, early examples have a disproportionate influence on the outcome of the training procedure. Even so, it is still somewhat unclear why that should be the case.

While there has been much research into the strengths and applications of deep belief networks and stacked denoising autoencoders specifically, there does not appear to have been any experiment to investigate the effect of unsupervised pre-training on cross-modal generalization performance of DBNs or SDAs.
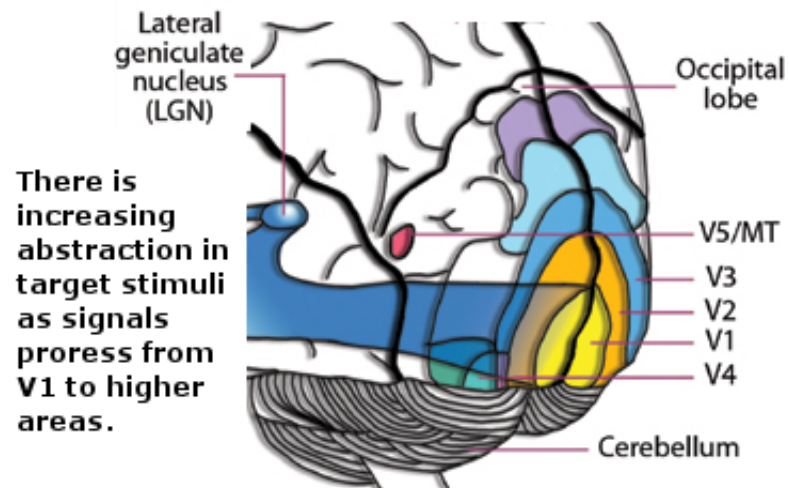
Figure 1: An illustration of the areas within the visual cortex. The layers in a deep networks mimic the stages of processing in the visual cortex. From *On The Origin Of The Human Mind* by Andrey Vyshedskiy [36]
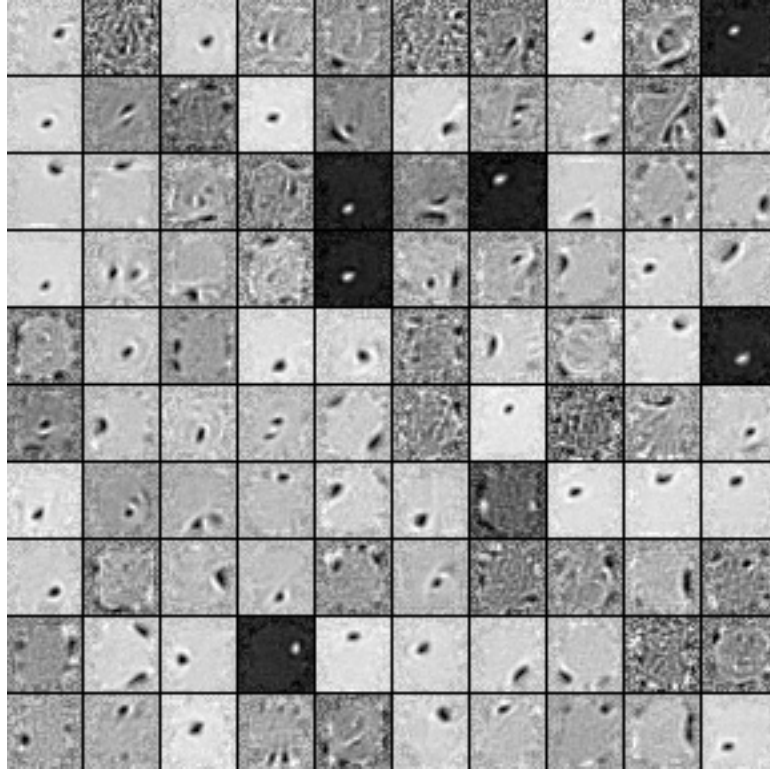
Figure 2: Edge, spot and gradient filters learned by a single denoising autoencoder. These are a common and efficient first level feature set for natural images. A feature is actually a set of weights, but an image can be generated to represent it, corresponding to the inputs that would produce a full signal on the given feature, and zero signal on all others. The extent to which these features resemble theoretical Gabor filters is an indicator of how well the model has generalized. This image was generated by me using the same code used in my main experiment. The model was trained on the MNIST digit recognition dataset.
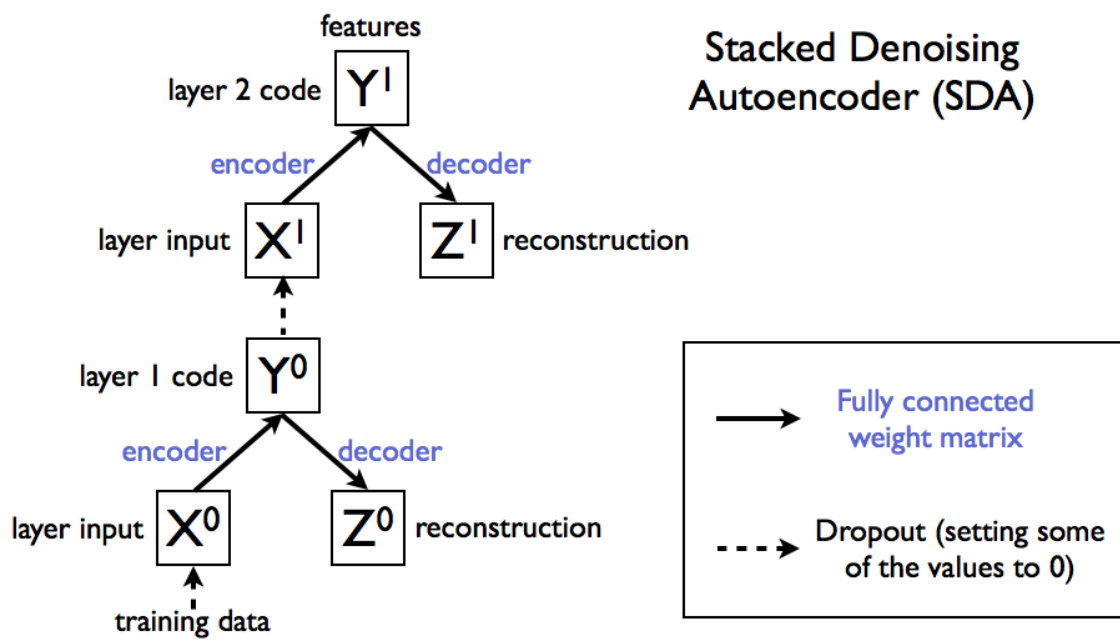
Figure 3: Stacked denoising autoencoder

2 Experiment design and implementation

2.1 Experiment Design

As described above, I test two distinct hypotheses in this thesis Firstly, that SDA models trained on one sensory modality and then switched to a second sensory modality half-way through training will have a higher reconstruction accuracy on test data from the second sensory modality than randomly initialized networks trained for an equal total number of epochs on the second sensory modality exclusively. In order to test this, I initialize an a pair of SDAs with three DA levels each. I train the experimental model for 249 epochs on audio, then on images for 249 epochs. I then measure its reconstruction accuracy on the image test set. For the control model, I initialize the same network and train it only on images for 498 epochs. I then measure its reconstruction accuracy on the image test set. The reconstruction accuracy on the test set is then compared between these two models. It is expected to be higher for the multi-modal (experimental) model because the more varied initial data will force it to generalize better than the control. This experiment is then repeated with the modalities reversed, and models' reconstruction accuracy on the audio test set is compared. This is 4 experiments in total.

For the second hypothesis, I run the four experiments just described using greedy layer-wise pre-training and without. The magnitude of the difference in reconstruction accuracy described in hypothesis 1 is expected to be greater for SDA's trained with greedy layer-wise pre-training. I refer to the control for hypothesis 2 as the interleaved models because the layers are trained in the following order: {123123...} Each time one layer is trained, it is called an epoch. During any given epoch, only one layer's weights are optimized. Every datum in the training set is used once during each epoch. The experimental models, also called the layer-wise models, the layers are

trained in the following order: {111...222...333...}. The number of epochs for each layer (166), and in total (498), is the same between the control and experimental models. For layer-wise models which are trained on both sensory modalities, all three layers are trained for each modality, totaling six groups of 83 epochs, three for one modality, then three for the other.

To summarize the experiment design, there are two types of training procedure needed to test hypothesis 2 (layer-wise and interleaved), there are two data source groups to test hypothesis 1 (single modality, and multiple modality), and there must be two experiments to control for the advantage given by training order (sound or images last). This gives 8 total models trained, as tabulated below and in Figure 6.

Summary of Experiments

1. Interleaved model on images only

2. Interleaved model on audio, then images

3. Layer-wise on images only

4. Layer-wise model on audio, then images

5. Interleaved model on audio only

6. Interleaved model on images, then audio

7. Layer-wise on on audio only

8. Layer-wise model on images, then audio

2.2   Network Architecture

In all the models trained, I used an architecture of three denoising autoencoders with input widths: [1024, 256, 64]. The dimensionality of the hidden code of the

highest layer is 16. The dropout rate used was 0.3 across all experiments and all layers, meaning 30 percent of values in the input vector to any layers are set to zero. Dumitru Erhan et al. [10] found that the benefits of greedy layer-wise pre-training do not manifest until three or more layers are used, and that more than five layers does not give measurable added benefit to test accuracy and variance on the MNIST dataset, which is of similar size to the data I used. Their network architecture for the three-layer SDA was [1200,800,400]. They tested a variety of hyper-parameters as well, such as corruption rates ranging from 0.0 to 0.4, learning rates from 0.01 to 0.0005, and the use of tied weights. I used a learning rate of 0.001 across all layers, and did not use tied weights.

2.3   Learning methods

Training an SDA is performed by training the component DA's in the prescribed order, depending on whether it is layer-wise or interleaved. Training a DA is very similar to training a classical neural network. A cost function is defined in terms of a given training example, and a pair of weight matrices, the encoder and the decoder. The training example is first corrupted according to the dropout rate, then it is multiplied by the encoder weight matrix, and passed through a sigmoid activation function to obtain the hidden code. The hidden code is then multiplied by the decoder matrix, and again through a sigmoid activation function to obtain the reconstruction. The distance between the reconstruction and the original uncorrupted input vector is the cost. Once a cost function is defined, any standard optimization procedure can be used to optimize the weights to minimize it. When the derivative of that function can be estimated or defined, a more powerful class of optimization algorithms is available. In the case of neural networks, the derivative is available, so Stochastic Gradient Descent (SGD) can be used to optimize the weights.

2.4 Implementation

The experiments reported in this thesis, and the data pre-processing programs were all written in Python 2.7. The code is open source and available on Github[30]. I based my implementation of the SDA algorithm on code and documentation written by the Theano Development Team. Theano is a Python library that allows the development of GPU accelerated linear algebra operations. It works with the commonly used scientific and numerical computing package Numpy. The SGD optimization for these experiments comes from Scikit Learn, a machine learning package for Python.

2.5 Data Preparation

The image dataset comes from the MIRFLICKR-1M collection of 1 million images from Flickr, all licensed under Creative Commons by their original authors. Flickr credits the authors on the MFLICKR description page [22]. For this experiment, 32 by 32 pixel normalized greyscale patches were desired. In preliminary experiments I determined that this is about the largest patch size I can use and still finish the experiment in about 12 hours, which is a reasonable turnaround time to work with. The patches are normalized because it helps neural-network based algorithms converge faster. At the standard 4 megapixel resolution of the example images, 32 by 32 pixel patches are smooth and relatively featureless, so 100 by 100 pixel patches were randomly sampled from the images in dataset and resized using bilinear interpolation to 32 by 32 pixels, and then desaturated. For the best results with neural networks, the brightness is represented as a floating point value between 0 and 1. No locality is preserved. The patch is flattened into a vector of width 1024. Every pixel is equally distant to every other from the perspective of the neural network. The network is expected to *learn* the correlations that exist between neighboring pixels. The data

are then normalized with ICA whitening (a kind of local contrast enhancement that has nothing to do with actually making the image whiter). This pre-processing step typically improves the convergence time and quality of learned features with neural networks. Whitening is essentially normalizing the data along the dimensions of greatest variation, as indicated by independent component analysis (ICA) The whitening procedure requires having the whole dataset up front, and therefore precludes use in on-line learning environments, however it is probably possible to adapt the algorithm to on-line learning with only some loss of accuracy. All my code is in Python and based on Numpy arrays, so I used the ICA functionality from scikit-learn, a machine learning package for Python.

Both the image and audio datasets are divided into training, test, and cross validation sets. 80% of each set is used to created the training set, 16% is used to create the test set, and 4% is used to create the cross-validation set. There are 100,000 vectors in each dataset before splitting. Each has a dimensionality of 1024 and is represented with 32-bit floating point precision. The training, test, and validation sets are each randomized by sorting over the Murmur3 hash of their indices with a large fixed offset which can be used as a random seed. This is one source of stochasticity in the experiment, the other being the randomly initialized weights for the network.

To the best of my knowledge there is no comparably rich, large, and well packaged audio dataset released under Creative Commons or in the public domain, so for my experiments I am using a collection of publicly aired talk-show broadcasts from which short clips are sampled and transformed into spectrograms of comparable dimensions to the image patches. The "patches" of spectrogram are 500 milliseconds long, divided into 32 time bins. They are also divided into frequency bins of 32 peak frequencies on a logarithmic scale with the lowest frequency peak being 50 hz and the highest being 10 khz. An equal number of samples were prepared from each sensory modality, images and sounds, and each datum is of the same dimensionality, and is normalized
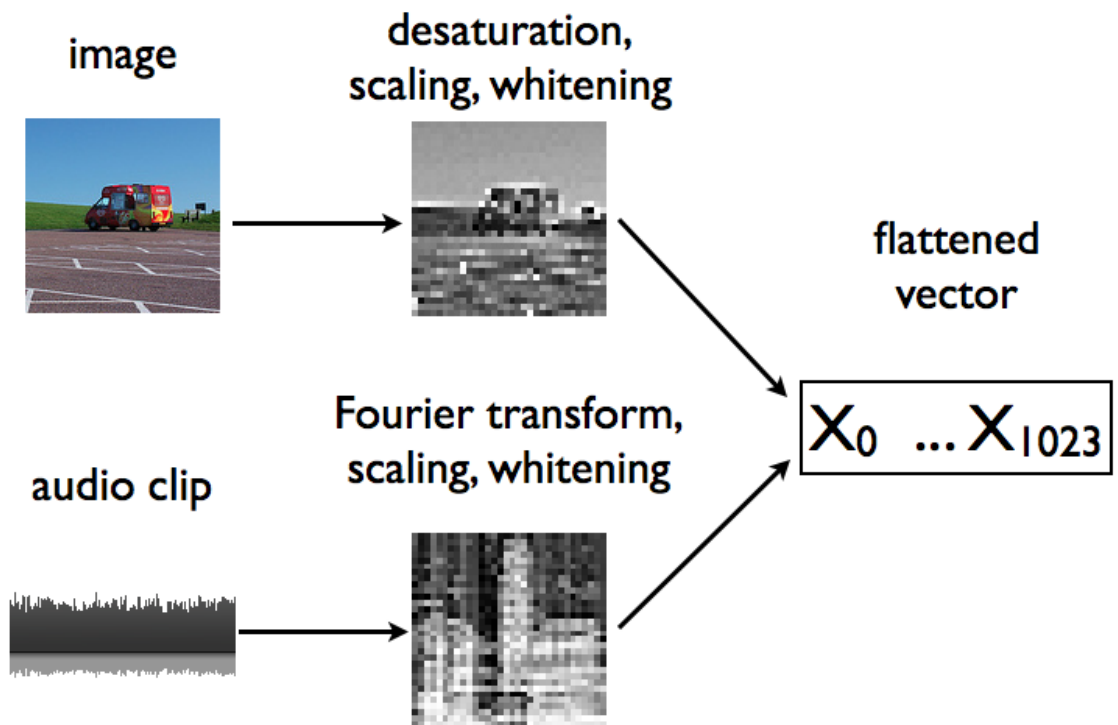
Figure 4: The data from both sensory modalities is preprocessed to create vectors of the same dimensionality to use as input to the learning algorithms.
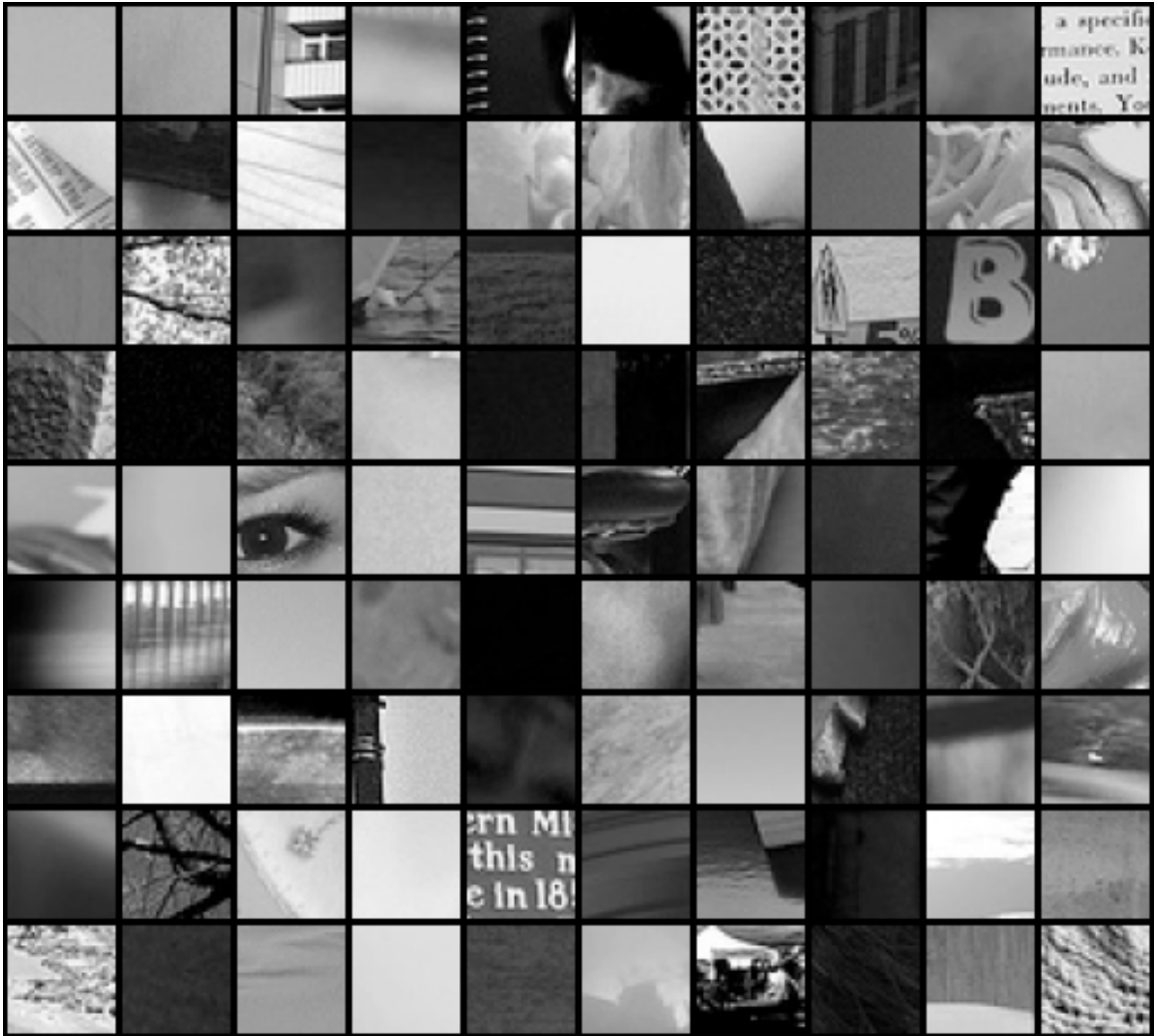
Figure 5: Patches sampled from the Flickr-1M dataset prior to whitening

in the same way. This way they can all be treated interchangeably, simplifying the code, and ensuring that any differences in learning between the two datasets are due to the differences in the content of their data, and not, for example, a different network topology for data of different dimensions.

Reconstruction Error of Models Trained

	Audio First	Images First	Same Throughout
with GLWPT	**94.5%** expected to be same as the cell to the right	**95.0%** expected to be higher than cells to right and below	**93.8%** expected to be higher than the cell below
SDG only	**94.0%** expected to be same as the cell to the right	**94.8%** expected to be lower than the cell to the right	**93.7%** baseline
	Multiple Modalities		Single Modality

Figure 6: The reconstruction accuriacies of test examples for each model after a total of 1 thousand training epochs each. There are 80,000 examples in the training set, and 16,000 examples in the test set.

3 Results and Conclusion

3.1 Experimental results

Hypothesis 1 is that networks pre-trained on one sensory modality performed better on the other modality than randomly initialized networks trained for an equal total number of epochs. To determine whether this has been confirmed I compare the reconstruction error from pairs of experiments where one was single-modal and the other was multi-modal, but the other variables were constant. There are four pairs: (1,2), (3,4), (5,6), and (7,8). The reconstruction errors are plotted in figure 7. Cross modal initialization seems to have helped for models which were tested on audio, but actually hindered performance on models which were tested on images. For each pair in the figure, the second box plot (multi-modal models) is expected to lie completely to the left of it's single modal counterpart.

The second hypothesis is that the magnitude of improvement gained from cross-modal initialization is greater when GLWPT is applied than when it is not. I found that it was only greater for models tested on audio. For models tested on audio (Experiments 5,6,7, and 8), layer-wise pre-training increased the improvement from cross-modal initialization, and in the case where cross-modal initialization hindered performance (Experiments 1,2,3 and 4) layer-wise pre-training lessened the amount it hindered.

When training any unsupervised learning algorithm, it is difficult to know whether the network has succeeded in learning the representations one expects. Measuring reconstruction error on test data gives an indication of how lossless the compression performed by the network is, but the goal is not perfectly lossless compression, it is generalizability and the discovery of interesting salient features that are useful to higher levels and similar networks. This is why it is crucial to visualize the features in
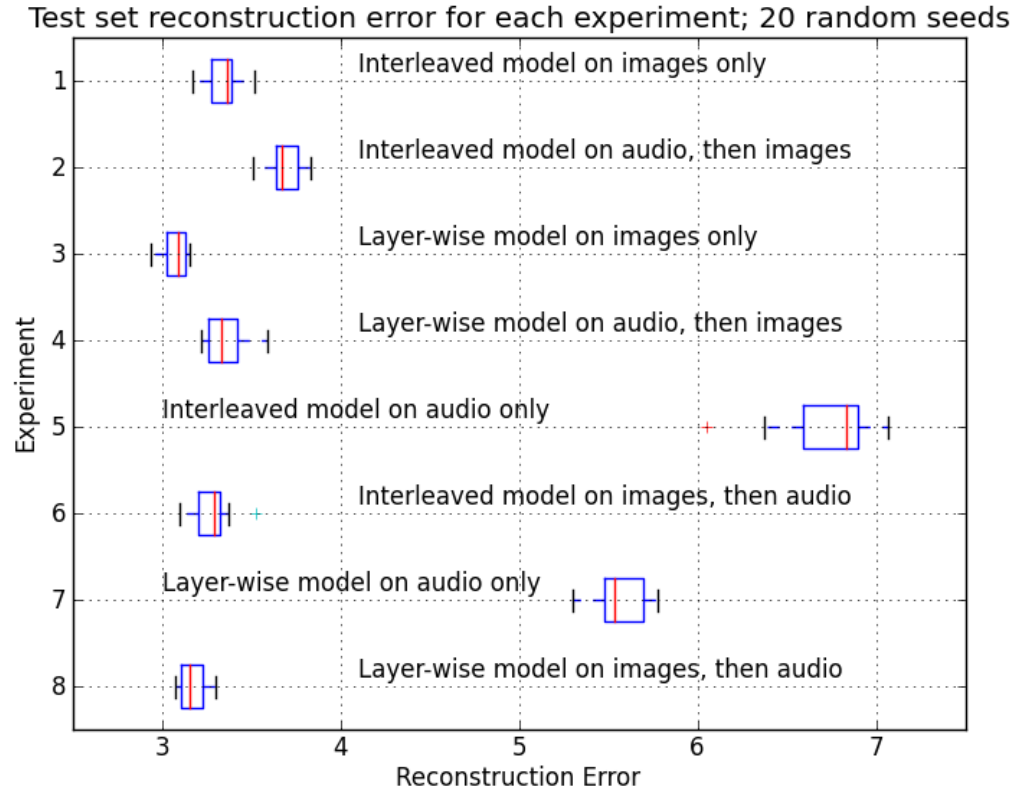
Figure 7: Box plots of the reconstruction error for each of the 8 experiments. Lower reconstruction error means better performance. A reconstruction error of about

the network. By working backwards from the weights, one can reconstruct an image that would maximally activate each node in a layer (figure 13). After performing this analysis on my networks, it seems that in all cases, about half of the nodes remain unused because they show no spatial correlation.

3.2 Conclusion

Reconstruction error across multiple sensory modalities is but one simple measurement that is analogous to neuro-plasticity. However, in the brain, plasticity is far more complicated and involves both modification of weights, and the alteration of the presence of network links and neurons. Likely, other unknown factors and limitations are involved as well. The experiments I have reported here indicate that a hierarchical representation alone is sufficient to allow a limited level of plasticity.

3.3 Future Work

References

[1] Yoshua Bengio. Learning deep architectures for ai. *Foundations and trends® in Machine Learning*, 2(1):1–127, 2009.

[2] Yoshua Bengio, Pascal Lamblin, Dan Popovici, and Hugo Larochelle. Greedy layer-wise training of deep networks. *Advances in neural information processing systems*, 19:153, 2007.

[3] Evgeny Byvatov, Uli Fechner, Jens Sadowski, and Gisbert Schneider. Comparison of support vector machine and artificial neural network systems for drug/nondrug classification. *Journal of Chemical Information and Computer Sciences*, 43(6):1882–1889, 2003.

[4] Minmin Chen, Zhixiang Xu, Kilian Weinberger, and Fei Sha. Marginalized denoising autoencoders for domain adaptation. *arXiv preprint arXiv:1206.4683*, 2012.
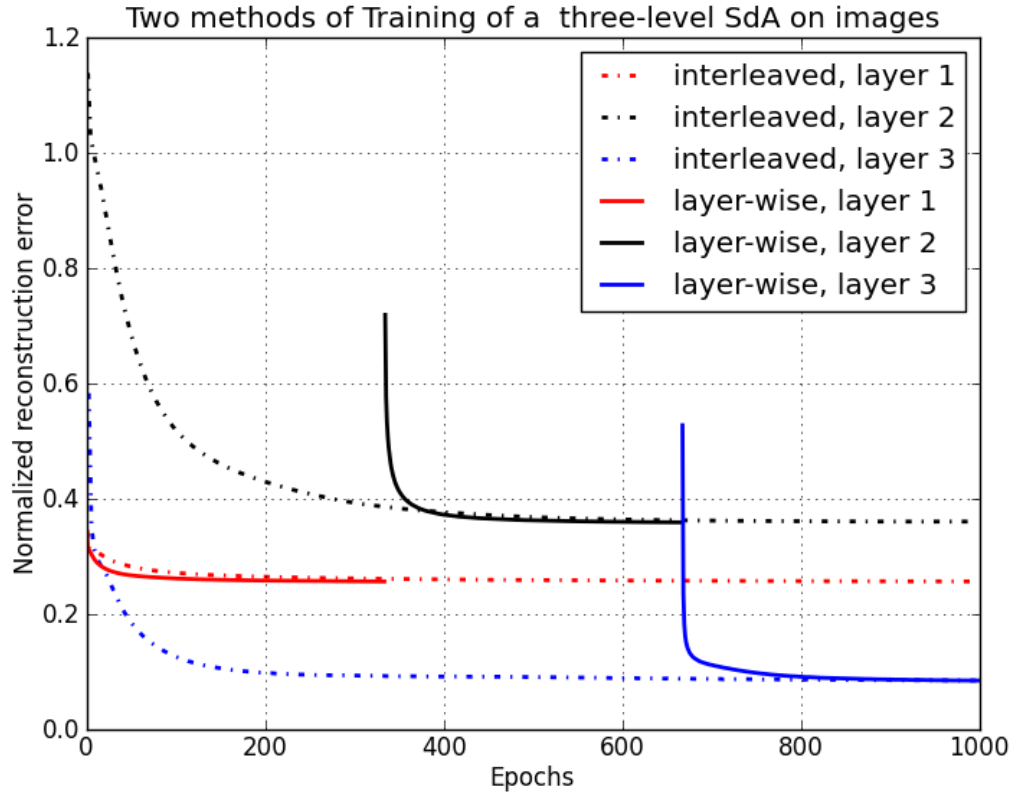
Figure 8: The control run, where an SDA is trained with both methods, on images. In both cases, the reconstruction error for each layer reaches about the same value. Interestingly, for images, the second level features have a higher reconstruction error than the 1st level features. One interpretation of this is that more of the information in images is encoded at this level. Please note that these graphs are best viewed in color.
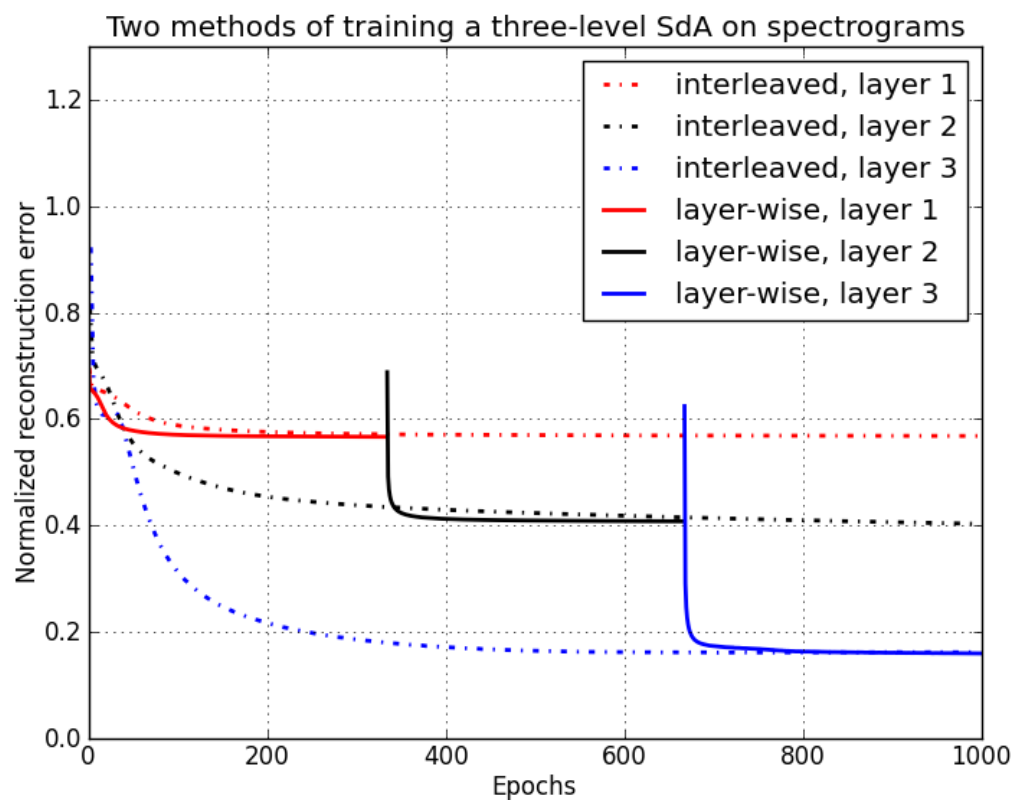
Figure 9: Second control run, with spectrograms. Unlike the images, the final normalized reconstruction error decreases with layer number. This could mean that these spectrograms have a flatter organizational structure, with more variability in the fine details, but less variability in which general structures are present.
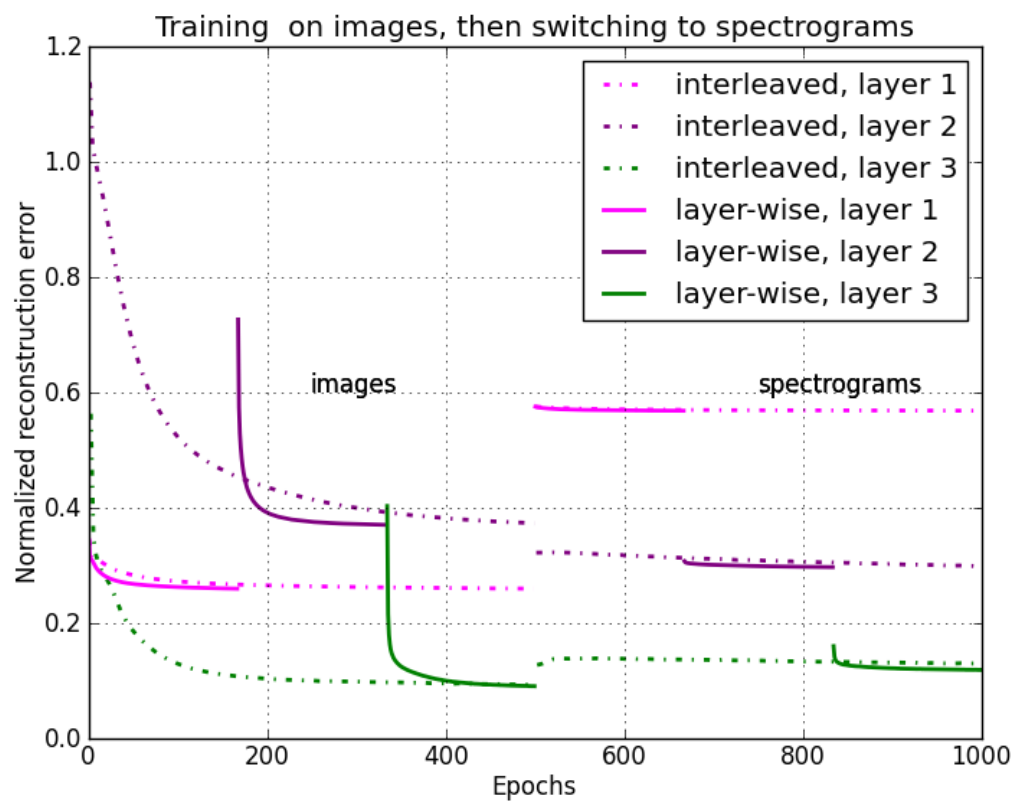
Figure 10: The first experimental run, in which models trained on images are switched to spectrograms on the 500th epoch. Note how the reconstruction error on spectrograms begins at roughly the value it would have stabilized at if the model were only trained on spectrograms, and deviates very little after that.
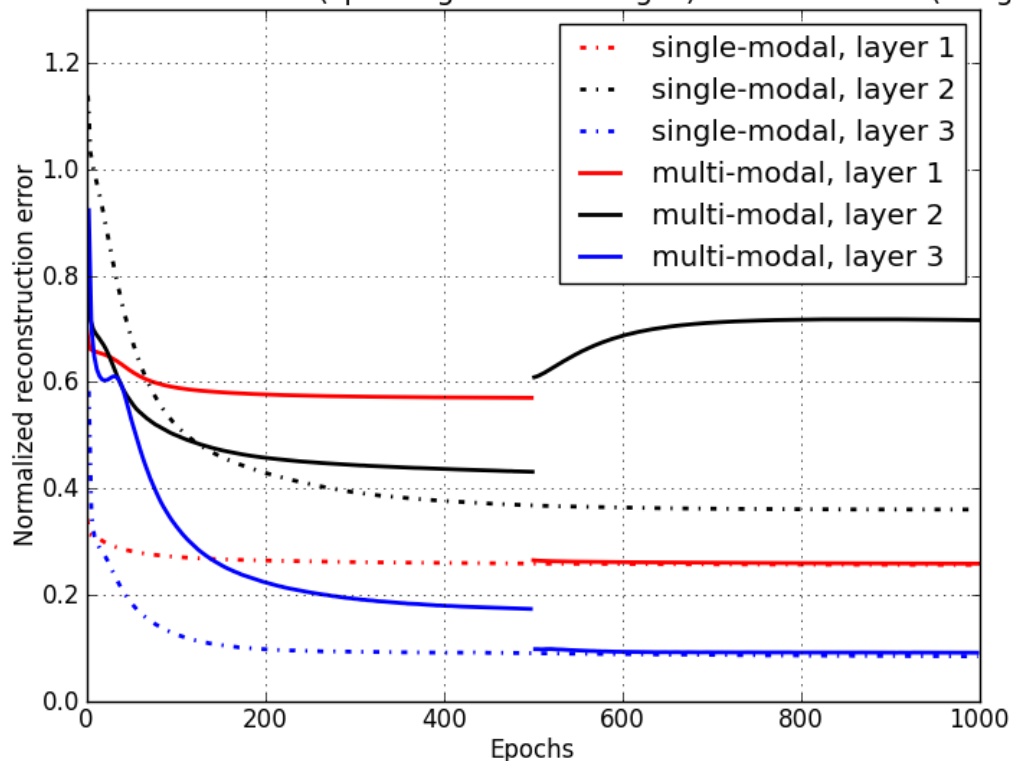
Figure 11: This graph compares a single interleaved network trained for 1000 epochs on images (dotted line) vs an interleaved network trained for 500 epochs on spectrograms, and then switched to images. Note the discrepancies between lines of the same color on the right half of the graph. The first and third layers see almost no change, but the second layer has two notable features. It begins in an unstable position, and then approaches a higher reconstruction error and stabilizes. This indicates that the structure of layer 1 is changing underneath it and altering it's fitness landscape, even which layer one's reconstruction error is stable.
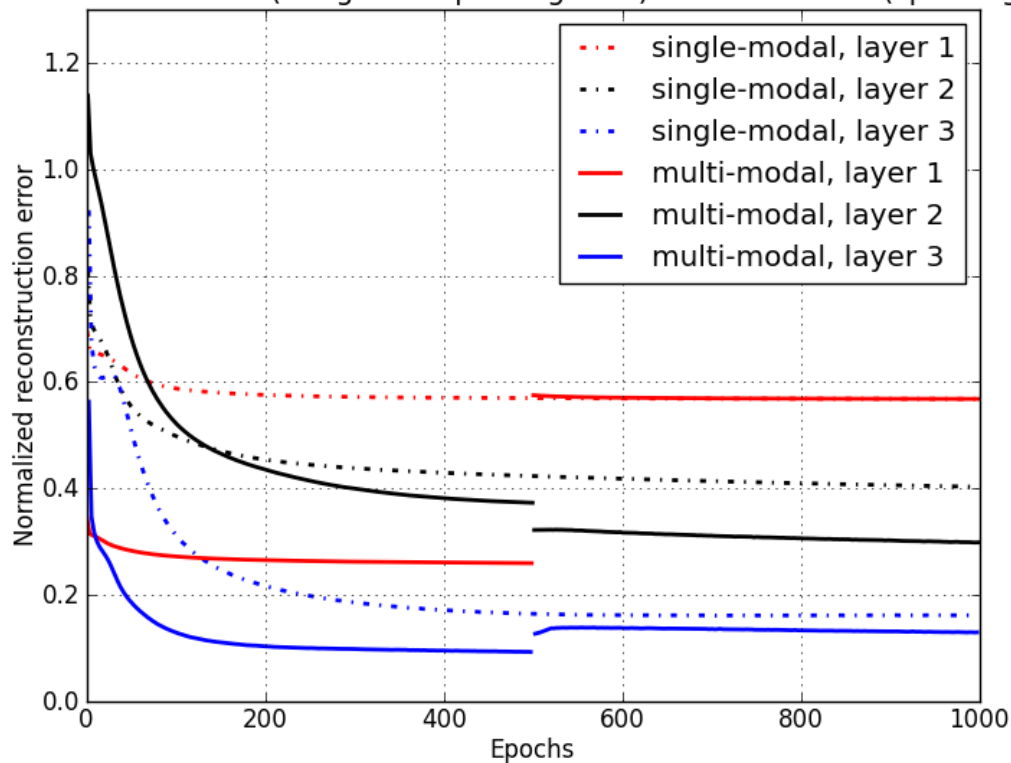
Figure 12: This graph, similar to the one above, compares a single interleaved network trained for 1000 epochs on spectrograms (dotted line) vs an interleaved network trained for 500 epochs on images, and then switched to spectrograms. (the modalities are opposite) The strangest feature of this graph is that the reconstruction error for layers 2 and 3 on spectrograms is lower for the network trained on images than the one trained on spectrograms. This indicates that images make good training data, even if the test data is not images.
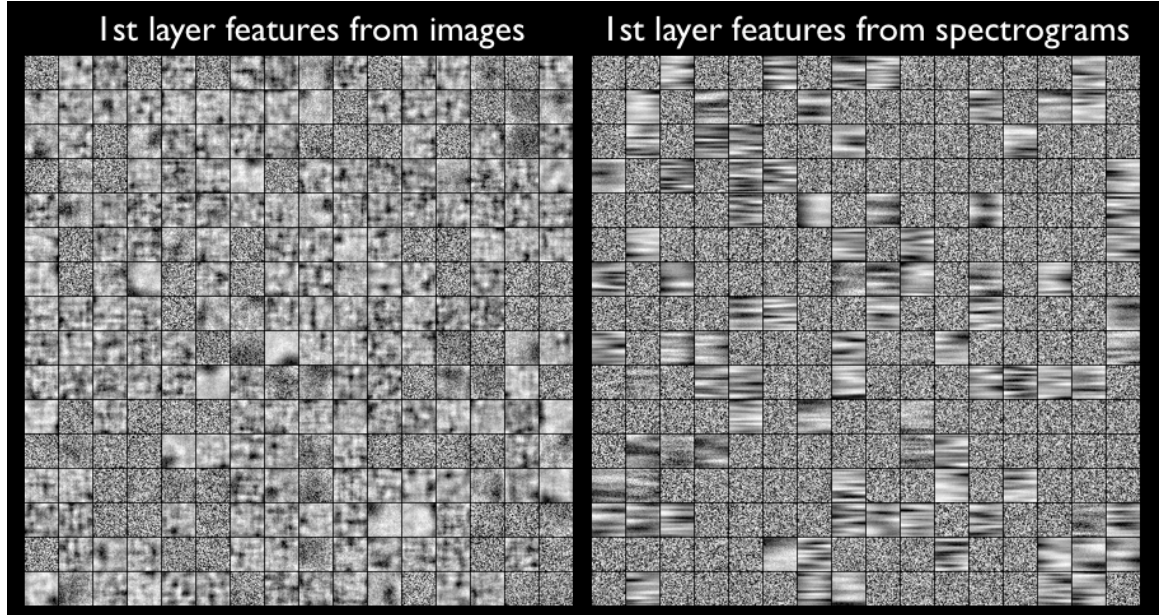
Figure 13: These grids of feature detectors are created by working backwards from the weights in the first-level denoising autoencoder to obtain the image which would maximally activate each node. If we compare visual representations of the first level features of the pure image network and the pure spectrogram network, we see that there are two main differences. In the image network, more of the features converge on smooth edge and spot detectors, whereas in the spectrogram network, fewer of the features are utilized. Any feature resembling uniform noise is basically not being used. The other difference is that the spectrograms appear stretched, because their vertical axis is frequency and the horizontal axis is time, the scale of features on these axes could be adjusted to be more like the images if desired.

[5] John G Daugman. Two-dimensional spectral analysis of cortical receptive field profiles. *Vision research*, 20(10):847–856, 1980.

[6] John G Daugman. Complete discrete 2-d gabor transforms by neural networks for image analysis and compression. *Acoustics, Speech and Signal Processing, IEEE Transactions on*, 36(7):1169–1179, 1988.

[7] J. Deng, W. Dong, R. Socher, L.-J. Li, K. Li, and L. Fei-Fei. ImageNet: A Large-Scale Hierarchical Image Database. In *CVPR09*, 2009.

[8] Chris HQ Ding and Inna Dubchak. Multi-class protein fold recognition using support vector machines and neural networks. *Bioinformatics*, 17(4):349–358, 2001.

[9] Dumitru Erhan, Yoshua Bengio, Aaron Courville, Pierre-Antoine Manzagol, Pascal Vincent, and Samy Bengio. Why does unsupervised pre-training help deep learning? *The Journal of Machine Learning Research*, 11:625–660, 2010.

[10] Dumitru Erhan, Pierre-Antoine Manzagol, Yoshua Bengio, Samy Bengio, and Pascal Vincent. The difficulty of training deep architectures and the effect of unsupervised pre-training. In *International Conference on Artificial Intelligence and Statistics*, pages 153–160, 2009.

[11] J. S. Garofolo, L. F. Lamel, W. M. Fisher, J. G. Fiscus, D. S. Pallett, and N. L. Dahlgren. DARPA TIMIT acoustic phonetic continuous speech corpus CDROM, 1993.

[12] Joshua Gluckman. Kurtosis and the phase structure of images. In *3rd International Workshop on Statistical and Computational Theories of Vision, Nice, France, October 2003 (in conjunction with ICCV03)*, pages 12–15, 2003.

[13] Alex Graves. Generating sequences with recurrent neural networks. *arXiv preprint arXiv:1308.0850*, 2013.

[14] Alexander Grubb and J Andrew Bagnell. Boosted backpropagation learning for training deep modular networks. In *Proceedings of the 27th International Conference on Machine Learning (ICML-10)*, pages 407–414, 2010.

[15] Jeff Hawkins. *On intelligence*. Macmillan, 2004.

[16] Geoffrey Hinton. Brains, sex, and machine learning. `http://www.youtube.com/watch?v=DleXA5ADG78`.

[17] Geoffrey Hinton, Li Deng, Dong Yu, George E Dahl, Abdel-rahman Mohamed, Navdeep Jaitly, Andrew Senior, Vincent Vanhoucke, Patrick Nguyen, Tara N Sainath, et al. Deep neural networks for acoustic modeling in speech recognition: The shared views of four research groups. *Signal Processing Magazine, IEEE*, 29(6):82–97, 2012.

[18] Geoffrey E Hinton. What kind of graphical model is the brain? In *IJCAI*, volume 5, pages 1765–1775, 2005.

[19] Geoffrey E Hinton, Peter Dayan, Brendan J Frey, and Radford M Neal. The" wake-sleep" algorithm for unsupervised neural networks. *SCIENCE-NEW YORK THEN WASHINGTON-*, pages 1158–1158, 1995.

[20] Geoffrey E Hinton and Ruslan R Salakhutdinov. Reducing the dimensionality of data with neural networks. *Science*, 313(5786):504–507, 2006.

[21] Geoffrey E Hinton, Nitish Srivastava, Alex Krizhevsky, Ilya Sutskever, and Ruslan R Salakhutdinov. Improving neural networks by preventing co-adaptation of feature detectors. *arXiv preprint arXiv:1207.0580*, 2012.

[22] Mark J. Huiskes and Michael S. Lew. The mir flickr retrieval evaluation. In *MIR '08: Proceedings of the 2008 ACM International Conference on Multimedia Information Retrieval*, New York, NY, USA, 2008. ACM.

[23] Anil K Jain and Farshid Farrokhnia. Unsupervised texture segmentation using gabor filters. *Pattern recognition*, 24(12):1167–1186, 1991.

[24] Alex Krizhevsky, Ilya Sutskever, and Geoff Hinton. Imagenet classification with deep convolutional neural networks. In *Advances in Neural Information Processing Systems 25*, pages 1106–1114, 2012.

[25] Hugo Larochelle, Dumitru Erhan, Aaron Courville, James Bergstra, and Yoshua Bengio. An empirical evaluation of deep architectures on problems with many factors of variation. In *Proceedings of the 24th international conference on Machine learning*, pages 473–480. ACM, 2007.

[26] Quoc V Le, Marc'Aurelio Ranzato, Rajat Monga, Matthieu Devin, Kai Chen, Greg S Corrado, Jeff Dean, and Andrew Y Ng. Building high-level features using large scale unsupervised learning. *arXiv preprint arXiv:1112.6209*, 2011.

[27] Honglak Lee, Roger Grosse, Rajesh Ranganath, and Andrew Y Ng. Convolutional deep belief networks for scalable unsupervised learning of hierarchical representations. In *Proceedings of the 26th Annual International Conference on Machine Learning*, pages 609–616. ACM, 2009.

[28] Honglak Lee, Yan Largman, Peter Pham, and Andrew Y Ng. Unsupervised feature learning for audio classification using convolutional deep belief networks. *Advances in neural information processing systems*, 2009.

[29] Srinivas Mukkamala, Guadalupe Janoski, and Andrew Sung. Intrusion detection using neural networks and support vector machines. In *Neural Networks, 2002. IJCNN'02. Proceedings of the 2002 International Joint Conference on*, volume 2, pages 1702–1707. IEEE, 2002.

[30] Nathan H. Nifong. Deep-planning codebase.

[31] Brandon Rohrer. Biologically inspired feature creation for multi-sensory perception. In *BICA*, pages 305–313, 2011.

[32] Ruslan Salakhutdinov, Andriy Mnih, and Geoffrey Hinton. Restricted boltzmann machines for collaborative filtering. In *Proceedings of the 24th international conference on Machine learning*, pages 791–798. ACM, 2007.

[33] Jitendra Sharma, Alessandra Angelucci, and Mriganka Sur. Induction of visual orientation modules in auditory cortex. *Nature*, 404(6780):841–847, 2000.

[34] Yichuan Tang, Ruslan Salakhutdinov, and Geoffrey Hinton. Deep lambertian networks. *arXiv preprint arXiv:1206.6445*, 2012.

[35] Pascal Vincent, Hugo Larochelle, Yoshua Bengio, and Pierre-Antoine Manzagol. Extracting and composing robust features with denoising autoencoders. In *Proceedings of the 25th international conference on Machine learning*, pages 1096–1103. ACM, 2008.

[36] Andrey Vyshedskiy. *On the Origin of the Human Mind: Three Theories; Uniqueness of the Human Mind, Evolution of the Human Mind, and The Neurological Basis of Conscious Experience.* MobileReference, 2008.